

COMPOSITIONAL VARIATIONS IN PLATINUM-GROUP MINERALS AND GOLD, KONDER ALKALINE-ULTRABASIC MASSIF, ALDAN SHIELD, RUSSIA

IVAN YA. NEKRASOV[†], ALEXANDER M. LENNIKOV[§], BORIS L. ZALISHCHAK,
ROSTISLAV A. OKTYABRSKY, VLADIMIR V. IVANOV, VALERY I. SAPIN[‡] AND VLADIMIR I. TASKAEV

*Far East Geological Institute, Far East Division, Russian Academy of Sciences,
159, prospect 100-letya, Vladivostok, 690022, Russia*

ABSTRACT

The platinum-group minerals (PGM) of the Konder zoned alkali-ultrabasic massif, located east of the Aldan Shield, in far-eastern Russia, are predominantly represented by isoferroplatinum of two generations, both with Fe contents ranging from 7.5 to 11.5 wt.%. A high-temperature isoferroplatinum is saturated with platinum-group-element (PGE) impurities: up to 5.3 Ir, 2.9 Os, and 1.8 Rh (all in wt.%). In contrast, the later isoferroplatinum contains lower levels of Ir, Os and Rh: less than 1.9 Ir, 1.0 Os, 0.6 Rh (in wt.%). The minor PGM are represented by a wide range of solid solutions in the system Os–Ir–Rh–Pt, tetraferroplatinum, tulameenite, hongshiite, minerals of erlichmanite–laurite and irarsite–hollingworthite series, sperrylite, bismuthides, antimonides, tellurides, stannides, and hydroxides. There are possibly new mineral species: native ruthenium, the Pd-dominant analogue of hongshiite, Pt₂As₃, the Pt-dominant analogue of konderite and inaglyite, and others minerals, which form rims around grains of isoferroplatinum and inclusions in it. A similar morphology and distribution as found with Pt₃Fe are observed with gold, related to rare lenses of sulfide and impregnations in dunite (Cu-, Pt-, and Pd-bearing high-grade gold) and monzodiorite cutting dunite (low-impurity middle- and low-grade gold).

Keywords: platinum-group minerals, gold, rare minerals, Konder massif, Aldan Shield, Russia.

SOMMAIRE

Les minéraux du groupe du platine provenant du complexe de Konder, ultrabasique, alcalin et zoné, situé à l'est du bouclier d'Aldan, en Russie orientale, sont surtout représentés par l'isoféropplatine, formé en deux générations, les deux ayant des teneurs en fer allant de 7.5 à 11.5% (poids). Une génération de haute température est saturée avec les autres éléments du groupe du platine sous forme d'impuretés: jusqu'à 5.3% Ir, 2.9% Os, et 1.8% Rh (base pondérale). En revanche, l'isoféropplatine tardif contient moins de 1.9% Ir, 1.0% Os, et 0.6% Rh. Parmi les minéraux accessoires du groupe du platine, on trouve une grande variété de solutions solides faisant partie du système Os–Ir–Rh–Pt, tétraferroplatine, tulameenite, hongshiite, minéraux des séries erlichmanite–laurite et irarsite–hollingworthite, sperrylite, bismuthures, antimoniures, tellurures, stannures, et hydroxydes. Les assemblages contiennent possiblement de nouvelles espèces minérales: ruthénium natif, l'analogue palladifère de la hongshiite, Pt₂As₃, et l'analogue platinifère de la konderite et de l'inaglyite, entre autres, qui forment des liserés autour des grains d'isoféropplatine et des inclusions dans cette phase. Nous observons pour l'or une morphologie et une distribution semblables à celles de l'isoféropplatine; l'or est lié à de rares lentilles de sulfures et des imprégnations dans la dunite (or de haute température, porteur de Cu, Pt, et Pd), et des venues de monzodiorite recoupant la dunite (or en moyenne ou faible teneurs, à faible contenu en impuretés).

(Traduit par la Rédaction)

Mots-clés: minéraux du groupe du platine, or, minéraux rares, complexe de Konder, bouclier d'Aldan, Russie.

[§] *E-mail address:* anortozit@mail.ru

[†] Deceased 2000.

[‡] Deceased 2001.

INTRODUCTION

The Konder alkali-ultrabasic massif, in far-eastern Russia, belongs to a set of platform analogues of the Ural–Alaska type of zoned platinum-bearing intrusive complexes (Cabri & Naldrett 1984). The accessory platinum-group minerals (PGM) from the primary and placer occurrences associated with the Konder intrusion are mainly represented by isoferroplatinum, as indicated by numerous electron-microprobe analyses and examinations by X-ray diffraction (Mochalov 1994, Nekrasov *et al.* 1994). Except in rare instances (Cabri & Laflamme 1997), reflections attributed to the superstructure were revealed in diffraction patterns of Pt₃Fe samples obtained in long-exposure studies (Mochalov 1994). These lines pertain to a primitive cubic cell. Claims of the widespread presence in the Konder massif of ferroan platinum having a disordered face-centered cubic cell (Razin 1978) have been called in question (Mochalov *et al.* 1988, Mochalov 1994).

Inclusions of Os–Ir–Ru and Os–Ir–Pt solid solutions are usually present in the isoferroplatinum. The minor minerals of the platinum-group element (PGE) are tetraferroplatinum, tulameenite, hongshiite, sulfides, sulfoarsenides, arsenides, bismuthides, antimonides, tellurides, stannides, Pd germanide, oxides and hydroxides, forming a rim around isoferroplatinum or incorporated as inclusions. Together with these minerals, accessory gold invariably occurs in outcrops and also in placers along streams draining the Konder massif.

Original results of a study of accessory PGE minerals in the Konder alkaline-ultrabasic massif are briefly described in this paper. More details are provided in a monograph of the authors (Nekrasov *et al.* 1994), which was published in a very limited number of copies (300). It became inaccessible almost immediately, even for Russian geologists studying PGM. Before of this monograph was published, all the information about the mineralogy of the noble metals in the Konder alkaline-ultrabasic massif was scattered in separate articles, either by the monograph's authors or by other specialists.

GEOLOGICAL SETTING

In addition to the Konder central-type massif with a dunite core, a few other concentrically zoned platinumiferous massifs of ultramafic and alkaline rocks are known in the central part of the Aldan Shield (Inagli) and in its southeastern part (Chad and Sybakh). All such massifs were formed at a depth of 1–2 km (Bogomolov 1964, El'yanov & Moralev 1972) and are eroded to some extent, giving rise to variable proportions of specific rocks exposed at the present-day surface (Nekrasov *et al.* 1994). The Sybakh and Inagli massifs are the least eroded, whereas the Konder and especially the Chad massifs are eroded to a greater depth.

The Konder annular alkaline-ultrabasic massif is located on the eastern margin of the Aldan Shield, in the

middle reaches of the Maya River, approximately 250 km northwest of the coast of the Okhotsk Sea (Fig. 1). Most of the massif is composed of ultrabasic rocks, represented by dunite, forming a rounded core about 6 km across. Olivine clinopyroxenite surrounds the dunite and grades to olivine-free magnetite-bearing pyroxenite, gabbro–pyroxenite, and further to melanocratic gabbro toward the periphery of the massif. The coarse-grained phlogopite-bearing magnetite clinopyroxenite occurs as dikes up to 40 m across in the southwestern sector of the dunite core. The dunite core and the enveloping pyroxenite contain numerous thin dikes (up to 1–2 m) of syenite and nepheline syenite. The enveloping clinopyroxenite is cross-cut in places by intrusive bodies of granodioritic, monzonitic or monzodioritic composition (Emel'yanenko *et al.* 1989, Nekrasov *et al.* 1994). According to geological data, the Konder intrusive body formed at a shallow depth (about 1.5 km) (Andreev 1987). No reliable evidence for the age of the Konder massif is available (Nekrasov *et al.* 1994, Pushkarev *et al.* 2001). The ultrabasic suite is considered to have formed not later than the Upper Proterozoic (Emel'yanenko *et al.* 1989, Shnai & Kuranova 1981), but the alkaline and monzonitic rocks may be partly of Mesozoic age (Emel'yanenko *et al.* 1989, Orlova 1991).

The contact aureole

Igneous rocks of the Konder intrusive complex have metamorphosed the enclosing Middle Riphean clastic sedimentary rocks. At the present-day level of erosion, the contact-metamorphic rocks are in the pyroxene-hornfels and muscovite-hornfels facies. In its outer part, the contact aureole, commonly more than 500 m across (Bogomolov 1964), is in the cordierite–biotite hornfels facies, with andalusite developed at the expense of sandstones and siltstones. The hornfels at the inner part of the contact aureole (more 100 m wide) were deformed owing to the intrusion of ultrabasic magma and also were subjected with acid leaching due to the late intrusion of granodioritic magma (Lennikov *et al.* 1991, Marakushev *et al.* 1990).

Associated carbonate rocks consist of periclase – forsterite – brucite marble and calc-silicate assemblages containing qandilite, the rare Ti–Mg spinel-group mineral (Oktyabrsky *et al.* 1992), as well as monticellite + melilite, vesuvianite + clintonite, grossular + diopside and scapolite-bearing varieties of skarn (Lennikov *et al.* 1991, Marakushev *et al.* 1990).

Petrography of the Konder massif

The dunite is a massive, fine- to medium-grained inequigranular rock, with olivine grains varying in size from fractions of a millimeter to tens of millimeters. Olivine crystals up to 5–7 cm in length can be seen in sporadic bodies of pegmatitic dunite. The fine-grained

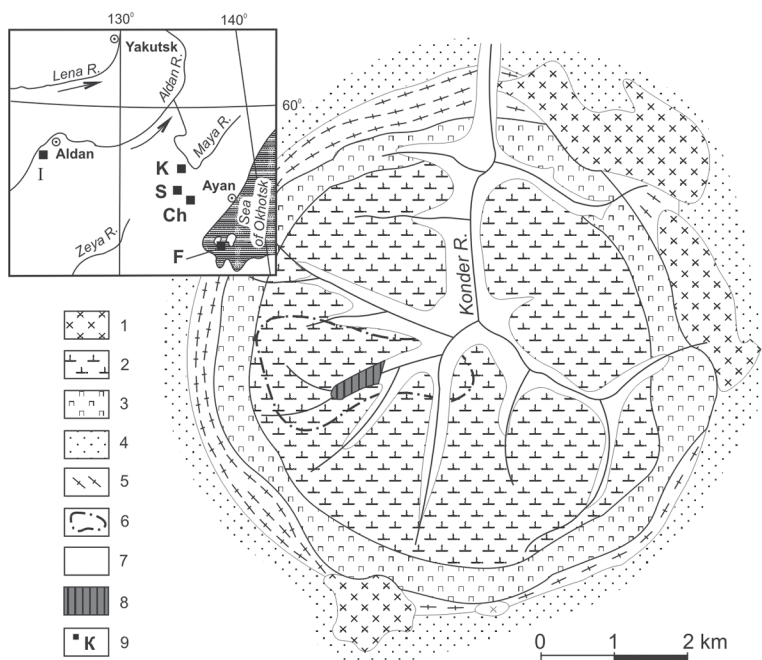


FIG. 1. Geological map of Konder alkali-ultrabasic massif, after Andreev (1987) and Sushkin (1995), with simplifications and additions. 1) Granodiorite, monzonite, monzodiorite; 2) dunite cut by dikes of syenite and nepheline syenite in the southern half of the dunite core; 3) olivine and magnetite-bearing pyroxenite with dikes of syenite and nepheline syenite; 4–5) massive (4) and gneissic (5) andalusite- and sillimanite-bearing biotite–cordierite hornfels formed at the expense of Riphean siltstones and sandstones; 6) area injected by phlogopite pyroxenite dykes; 7) platinum-bearing alluvium; 8) platinum–gold-bearing alluvium; 9) site of the Konder massif (K) and its associated bodies Inagli (I), Chad (Ch), Sybakh (S) and Feklistov (F).

dunite occurs in marginal parts of the core. The main body is composed of medium-grained dunite locally grading into a coarse-grained variety. According to the results of drilling, the coarse-grained dunite becomes predominant at a depth of more than approximately 200 m.

Olivine from the fine- and medium-grained dunite corresponds to $FO_{87.9-93.1}$ (Nekrasov *et al.* 1994). Olivine in clinopyroxene-bearing dunite from the marginal zone of the core is somewhat richer in Fe ($FO_{86.9-87.6}$). The pegmatitic dunite in the central part of the core and dunite inclusions in olivine clinopyroxenite contain $FO_{84.9-85.3}$ and $FO_{81.6-84.0}$, respectively. Schlieren of pegmatitic olivine clinopyroxenite hosted in dunite contain $FO_{87.3}$, whereas the composition of olivine in clinopyroxenite surrounding the dunite core and forming dikes therein attains FO_{70} .

The chromian spinel, abundant in dunite and olivine clinopyroxenite from the central part of the Konder massif, is largely composed of ferrian chromite, both

accessory and ore-forming. The accessory chromian spinel occurs as disseminated octahedra and, less commonly, flattened and rounded equant grains from 0.01 to 2–3 mm across. Rounded and lenticular schlieren, vein-like bodies and pockets (up to 0.7×1.5 m² across) of densely impregnated chromian spinel ore are distributed throughout the massif, without apparent systematic pattern in spatial distribution.

The chromian spinel is associated with $FO_{87.1-92.9}$ in dunite and $FO_{87.3-87.6}$ in olivine clinopyroxenite of the central facies. The chemical composition of the chromian spinel covers a range from a sporadically encountered high-Cr variety (61.7–63.7 wt.% Cr_2O_3 ; Rudashevsky & Mochalov 1985), via the main mass of ferrian chromite, to the Cr-bearing magnesian magnetite. The Cr content of the chromian spinel from dunite varies from 55.0 to 19.6 wt.% Cr_2O_3 in magnesian magnetite. In the magnetic fraction of densely impregnated chromian spinel, the respective ranges are 7.6–8.6 and 10–12 wt.% Cr_2O_3 (*i.e.*, chromian magnetite). The Mg

content varies to a lesser extent, from 3 to 11 wt.% MgO. The ore-zone chromite is distinguished by the highest Mg content.

The chromian spinel from dunite and olivine clinopyroxenite of the central facies contains an appreciable quantity of titanium. The lowest Ti content is typical of ore-zone chromian spinel, and the highest is found in octahedra of chromite (0.4–0.8, and up to 1.55 wt.% TiO₂, respectively). The accessory chromian spinel from pegmatitic and coarse-grained dunite and from olivine clinopyroxenite of the central facies is somewhat richer in Ti (1.07–1.95 wt.% TiO₂). The range in TiO₂ in Cr-bearing magnetite is narrower, but higher (1.80–2.12 wt.% TiO₂).

The chromian spinel from Konder is relatively poor in Al. The highest Al content (5.9–7.9 wt.% Al₂O₃) was detected in the ore-zone chromian spinel and accessory spinel of the first generation in dunite. The Al content of chromite from the pegmatitic olivine clinopyroxenite and from the fine-grained rocks drops to 5.2–3.3 and from 4.6–2.4 to 0.8 wt.% Al₂O₃, respectively. The Al content in the Cr-bearing magnetite (1.8–2.5 wt.% Al₂O₃) and densely impregnated chromite schlieren in dunite (1.97–2.49 wt.% Al₂O₃) varies over approximately the same range.

Clinopyroxene of the ultrabasic suite of the Konder massif is distributed as widely as the chromian spinel. Within dunites, it forms schlieren-like accumulations and thin veinlets, but in the pyroxenites, it is a rock-forming mineral.

The pyroxene in the intercalated suite of dunites and olivine pyroxenites of the central facies, as in the magnetite-free pyroxenites of the ring unit, is low in ferrous iron ($4.5 < f_{\text{total}} < 20.6\%$) [$f_{\text{total}} = 100(\text{Fe}^{2+} + \text{Fe}^{3+})/(\text{Mg} + \text{Fe}^{2+} + \text{Fe}^{3+})$], moderately aluminous (0.5–2.2 wt.% Al₂O₃) and low in titanium (0.1–0.44 wt.% TiO₂). It is enriched in Cr (0.25–0.76 wt.% Cr₂O₃).

The clinopyroxene in magnetite-bearing pyroxenites and within dikes of pyroxenite in dunite contain significantly more Ti (to 1.14 wt.% TiO₂) and less Cr (0.1 wt.% Cr₂O₃), but is more ferrous (f_{total} to 30%) and moderately aluminous (to 2.4 wt.% Al₂O₃). A characteristic feature of the ring clinopyroxenites of the Konder massif is the high value of the oxidation ratio ($48 < f_o < 56\%$) [$f_o = 100\text{Fe}^{3+}/(\text{Fe}^{2+} + \text{Fe}^{3+})$], which is evidence of the presence of the aegirine end-member; the pyroxene contains up to 0.85 wt.% Na₂O.

The clinopyroxenite in dikes cross-cutting dunite at the southwestern part of the core of the complex differs from ring clinopyroxenites by their significantly lower Cr content (0.02 wt.% Cr₂O₃) and by the greater proportion of ferrous iron ($20 < f_{\text{total}} < 23.5\%$). In these pyroxenites, opaque minerals along with apatite are represented by titaniferous magnetite (4.7–5.8 wt.% TiO₂), in some cases intergrown with oxidized (5.9–8.8 wt.% Fe₂O₃) ilmenite with appreciable Mg (3.7–3.8 wt.% MgO) in solid solution, with pyrrhotite and chalcopyrite.

As for the dikes of clinopyroxenite, they can be subdivided according to the minerals present into phlogopite-, hornblende- and magnetite-bearing varieties. Large (up to 2 mm) red-brown single crystals of vesuvianite and faintly pink xenomorphic grains (1–2 mm) of titanite are present within the coarse-grained units.

The formation of the dunite core was completed by crystallization of native metals (Si-bearing and pure α -iron, tin, copper, and antimony), along with rare grains, polymineralic veinlets and lenses of pentlandite, pyrrhotite, chalcopyrite, pyrite, and arsenopyrite.

ANALYTICAL TECHNIQUES

The PGM were analyzed quantitatively with a JXA-5A electron microprobe under the following conditions: acceleration voltage 25 kV, beam current 30 nA, counting time 10 seconds. We used the *L* series of X-ray lines and pure metals as standards. Concentrations of elements other than the PGE were determined using the following X-ray lines and standards: *SK* α , *BiL* α , *M* α : Bi₂S₃; *FeK* α : FeS₂; *CuK* α , *SbL* α : CuSbS₂; *SnL* α : SnO₂; *NiK* α , *AuL* α , *AgL* α , *GeL* α : pure elements; *PbL* α , *M* α : PbS; *SeK* α , *L* α : Zn, Se; *HgL* α : HgS; *TeL* α : Cd, Te; *AsK* α , *L* α : FeAsS. Overlaps of X-ray lines (Laputina 1980) were taken into account with a correction program using the relative intensities of X-ray lines. The detection limit for PGE is 0.1–0.3 wt.%. The precision of analyses was evaluated on PGM with a stoichiometric composition, and deviations were at the 2–3% limit in the most cases. Analyses were made by V.I. Sapin and V.I. Taskaev; a dash indicates that the element was not detected. The proportion of the elements is expressed in wt.%.

PGE MINERALS OF THE KONDER MASSIF

According to the results of prospectors' activities (Sushkin 1995), the major portion of the platinum-rich heavy-mineral concentrate consists of irregular, lump-shaped, angular, and perfectly faceted grains of variable dimensions, up to nuggets (that weigh more than 10 g). Euhedral crystals of platinum mainly are cubic in habit. Hexahedral crystals dominate in small-size fractions. The proportion of various twins and intergrowths of two or three individuals, up to 17 mm in dimension, increases among coarser grains. Films of gold, 0.05–1.0 mm thick, surround many small grains of platinum. In some cases, these films are coupled with a crystalline gold dust. The gold films are without doubt endogenic, because they consist of closely intergrown tiny crystals of Cu-bearing gold, Au- and Te-bearing sulfide, and some Pd and Pt compounds. The films on crystal edges are abraded during transport, and thus provide additional morphological evidence for their relatively high-temperature origin (Sushkin 1995). However, the micrometer-thick gold films of high fineness on rounded platinum nuggets most likely are of low-temperature

origin (Nekrasov *et al.* 1994). Native gold, silver, lead, tin, copper, nickel, iron, antimony and bismuth occur along with platinum in both bedrock and stream placers (Emel'yanenko *et al.* 1989).

More than 50 PGE, Au- and Ag-bearing minerals, including new and rare species, were identified in loose sediments over 20 years of systematic study of noble-metal mineralization. Discovery of new PGE minerals continues to this day (Shcheka *et al.* 2004). Many of these minerals were also detected in bedrock. The specific assemblages of minerals are related to one of two principal sources of platinum: chromite-bearing dunite in the core of the massif and the adjacent clinopyroxenite, and dikes of phlogopite–magnetite clinopyroxenite that intrude dunite and spatially associated sulfide lenses in the southwestern part of massif. Other PGM occur in extremely small quantities as tiny (commonly, no larger than a few tens of micrometers), globular and tabular inclusions within platinum and as an outer rim around these grains. Segregations of such phases are extremely sporadic. Nevertheless, these micro-inclusions turn out to be very diverse and attract the most interest.

Isoferroplatinum and ferroan platinum

Isoferroplatinum, the main PGM, is very heterogeneous in terms of amount of iron and the other PGE. Two varieties of this mineral were identified in the chromite-bearing dunite of the Konder massif (Nekrasov *et al.* 1991b): an early, high-temperature variety in association with chromite accumulations (up to 64 wt.% Cr_2O_3) and Mg-rich olivine (6–9% Fa), and a late variety that fills the interstitial space in lenses and veins of massive chromitite (up to 54 wt.% Cr_2O_3). Forsterite (Fo_{94-95}), chromian clinopyroxene, chromian amphibole, Cr–Na-bearing phlogopite, chromite inclusions are commonly included in the isoferroplatinum (Rudashevskiy *et al.* 1982). The early isoferroplatinum is relatively rich in other PGE and characterized by a variable Fe content, from 7.5 to 11.5 wt.% (24–35 at.%) that decreases with depth (Table 1, Fig. 2). Inclusions of Os, Ir, Ru, and Pt minerals are typical. In contrast, the late Pt–Fe alloy is free of such inclusions and is depleted in other PGE (except Pt), retaining the same Fe content (Table 1).

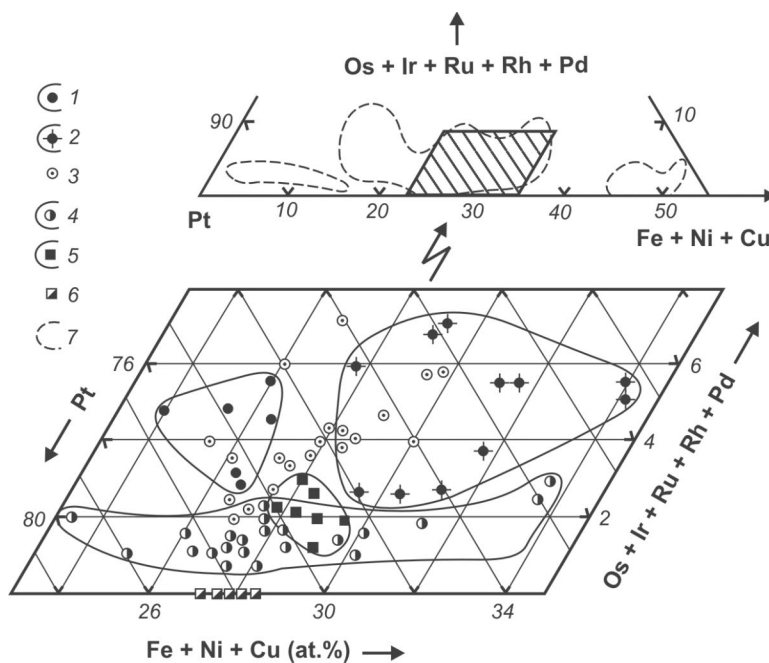


FIG. 2. Composition of native accessory isoferroplatinum from chromite-bearing dunite of more (1) and less (2) eroded and other (3) parts of the dunite core of the Konder massif; massive chromite veins and schlieren in dunite (4), and ferroan platinum from phlogopite–magnetite pyroxenites (5), forming dikes in dunite (Table 1), and from cubic nuggets of platinum (6) locally coated with a film of Cu-bearing gold (after Cabri & Laflamme 1997, Shcheka *et al.* 2004). Contours of fields of native Pt–Fe solid solutions from chromite-bearing dunite of ultramafic formations (7) are shown (after Zhernovskiy *et al.* 1985).

The ferroan platinum from dikes of phlogopite–magnetite clinopyroxenite that intrude dunite typically consists of cubic crystals locally coated with a film of Cu-bearing gold. The level of PGE impurities in the cubic crystals is close to that in isoferroplatinum in the late Pt–Fe alloy, but the iron content is higher (Fig. 2): 9.5–11.5 wt.% Fe (27–30 at.%). Amphibole, calcic clinopyroxene, aegirine-augite, aegirine, phlogopite, magnetite and apatite inclusions are common in the ferroan platinum (Shcheka *et al.* 2004).

In the Konder massif, in which the depth of erosion in dunite reaches 350–400 m (Nekrasov *et al.* 1994), the maximum Fe content (up to 11.5 wt.%) in the Pt–Fe solid solution is encountered in the uppermost part of the massif. In the isoferroplatinum associated with chromite accumulations, found in the deepest levels of the dunite body, the Fe content falls to 8–9 wt.%. The content of other PGE impurities in the Pt–Fe alloy shows a dependence on depth of crystallization. In the least eroded areas of the dunite, isoferroplatinum contains (wt.%): 0.8–3.8 Ir, up to 2.9 Os, up to 1.5 Pd, and 0.5–1.8 Rh; in the most deeply eroded zone of the dunite, it contains 2.5–5.3 Ir, 0.7–0.9 Os, 0.2–1.0 Pd, and 0.7–1.1 Rh. The PGE contents in isoferroplatinum show intermediate values in the other parts of the massif.

TABLE 1. COMPOSITION OF ISOFERROPLATINUM AND FERROAN PLATINUM, KONDER ALKALI-ULTRABASIC MASSIF, RUSSIA

No.	Pt	Ir	Os	Pd	Rh	Ru	Cu	Ni	Fe	Total
Dunite with accessory chromite–isoferroplatinum impregnations										
A. The least eroded zone of the massif										
1	84.59	3.03	1.17	0.45	1.18	0.13	0.75	0.43	9.70	101.43
2	84.46	0.76	2.64	1.51	0.77	-	1.65	0.36	9.25	101.40
3	84.74	0.88	2.86	1.44	1.03	-	1.72	0.38	9.25	102.30
4	85.65	1.94	0.57	-	-	-	0.12	-	10.97	99.25
5	80.39	3.37	-	-	1.66	0.14	1.06	0.83	11.47	98.92
B. The most eroded zone of the massif										
6	86.57	1.87	0.89	0.90	0.76	-	0.69	0.37	8.27	100.32
7	87.09	1.74	0.72	0.99	0.68	-	0.52	0.13	8.03	99.90
8	83.36	5.28	-	-	0.85	-	0.50	-	8.77	98.76
9	85.51	2.22	-	0.20	1.06	-	0.36	-	9.26	98.61
10	86.87	1.95	-	0.53	0.41	-	0.70	-	9.00	99.46
Chromite segregations in dunite with accessory isoferroplatinum										
11	83.87	0.70	-	-	1.37	0.12	1.02	0.71	11.40	99.19
12	86.98	0.58	-	-	0.70	-	0.50	0.53	10.92	100.21
13	89.23	-	0.32	0.17	0.16	-	0.82	-	9.11	99.81
14	89.93	0.08	-	0.39	-	0.18	0.52	0.53	8.64	100.27
15	88.59	0.31	0.45	-	0.36	-	1.75	0.25	8.04	99.75
Pyroxenite (dikes in dunite) with accessory ferroan platinum										
16	87.07	0.41	0.27	0.33	0.56	-	0.48	-	10.27	99.39
17	87.46	-	0.33	0.37	0.23	-	0.71	-	10.04	99.14
18	87.71	-	0.43	0.58	0.47	-	1.00	-	9.56	99.75
19	88.02	-	0.30	0.61	0.54	-	0.77	-	9.50	99.74

Compositions are expressed in wt.%.

Os–Ir–Ru–Pt solid solutions

As the end member of two solid-solution series Os – Ir – Ru and Os – Ir – Pt, osmium is the more common; on the contrary, platinum and ruthenium are very rare (Table 2). Impurity-free platinum occurs in the Konder massif as isolated inclusions (10–15 µm) of isoferroplatinum and tetraferroplatinum grains, whose margins have undergone low-temperature alteration. It is associated with micro-inclusions of gold and aggregates of porous Pt-oxide (see below).

Impurity-free iridium (up to 30 µm) and ruthenium (30 × 170 µm) also form rare inclusions in isoferroplatinum. Ruthenium in the Konder massif was first noted by Nekrasov *et al.* (1993).

Osmium is the most commonly encountered, and exhibits one of three habits. It may form rare, predominantly laminar, and in some cases roundish or worm-like inclusions in cumulate isoferroplatinum of the first generation, enriched in PGE impurities. As a rule, this osmium has a high level of Pt and Ir, up to 6 and 17 wt.%, respectively. The second variety of osmium forms disk-shaped and roundish grains. It has a low level of Pt and Ir, less than 3 and 11 wt.%, and reveals a zonal distribution of Ir in the largest grains, with maximum Ir in the core. This variety of osmium forms inclusions in the low-impurity isoferroplatinum of the second generation. The third variety of osmium forms isolated lamellar aggregates of relatively coarse-grained osmium (50 × 350 µm) with a low level of impurities (up to 2 wt.% of

TABLE 2. COMPOSITION OF Os–Ir–Ru–Rh–Pt SOLID SOLUTIONS INCLUDED IN ISOFERROPLATINUM, KONDER ALKALI-ULTRABASIC MASSIF

No.	Pt	Ir	Os	Rh	Ru	Total
1	2.10	10.10	84.96	0.55	2.00	100.46
2	2.06	2.05	91.64	0.85	1.25	98.18
3	1.79	21.14	72.12	0.73	2.78	99.39
4	1.64	2.44	94.52	0.80	0.38	99.59
5	2.11	12.97	81.88	0.64	1.11	98.98
6	4.39	41.55	27.55	-	25.47	98.96
7	3.20	36.35	39.78	-	20.44	99.77
8	0.84	29.64	68.61	-	-	99.09
9	3.51	34.88	41.25	-	19.03	98.67
10	26.78	38.09	19.11	-	14.40	99.75
11	9.22	54.49	30.12	1.59	2.98	99.16
12	10.37	31.06	56.44	-	1.03	99.26
13	9.85	57.32	30.58	-	0.96	98.99
14	10.64	52.87	37.16	0.29	-	101.11
15	14.04	62.91	20.91	-	0.30	98.97
16	2.20	18.68	76.88	0.40	1.37	99.53
17	0.13	24.26	72.53	0.33	2.42	99.69
18	-	0.60	0.23	-	98.87	99.70
19	-	8.45	55.11	-	35.88	99.44

Note: a selection of the 56 compositions available (Nekrasov *et al.* 1994) is given. Additional determinations have been included in the totals: Pd in compositions 1 (0.28%), 2 (0.33%), 3 (0.13%) and 4 (0.33%); Cu in compositions 1 (0.19%), 3 (0.25%), 5 (0.27%), 11 (0.50%) and 17 (0.15%); Fe in compositions 1 (0.12%), 3 (0.45%), 10 (1.37%), 11 (0.26%), 12 (0.36%), 13 (0.28%), 14 (0.15%) and 17 (0.12 wt.%).

Ir, Pt); it fills interstices in isoferroplatinum of the second generation.

In the Konder massif, solid solutions in the system Os–Ir–Ru–Pt consist mainly of compounds with Os or Ir dominant (Fig. 3), and are named in accordance with the nomenclature of Harris & Cabri (1991). Isolated grains of rutheniridosmine and ruthenium-dominant solid solutions with wide variability are present but rare. There are single occurrences of solid solutions whose compositions occupy the miscibility field. Such an anomaly may be the result of the influence of the Pt matrix during electron-microprobe analysis. It is possible that the field of miscibility of the compositions of natural Pt–Os–Ir and Ru–Os–Ir solid solutions is less

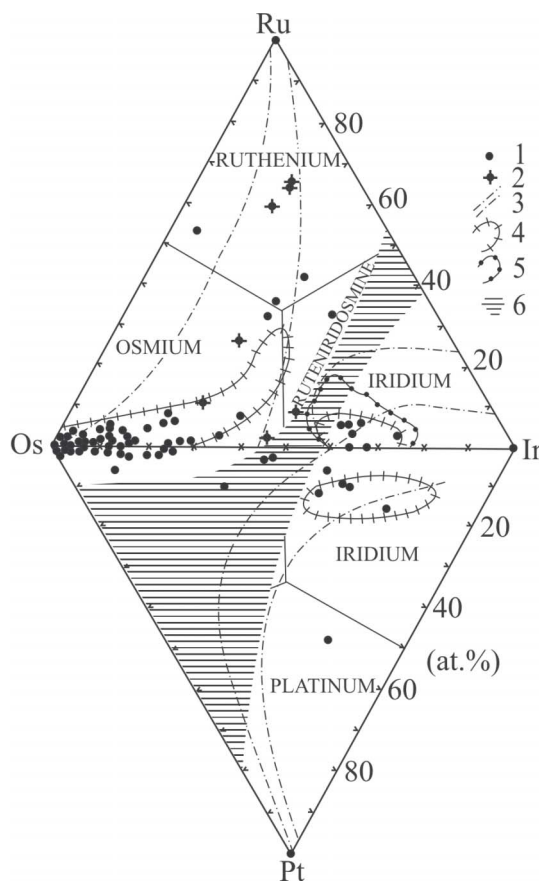


FIG. 3. Diagram representing solid solutions of Os–Ir–Ru–Pt system of Konder massif. 1) Data of Table 2, 2) after Mochalov (1994), 3) fields of solid-solution compositions of PGE from alpine-type ultrabasic rocks (after Dmitrenko *et al.* 1985), 4) the same from the massifs of alkali-ultrabasic formation (after Rudashevsky 1989), 5) the same from Konder massif (after Mochalov 1994), 6) miscibility gaps (after Harris & Cabri 1991).

significant, in agreement with the analytical data on alpine-type ultrabasic rocks in northeastern Russia (Mochalov 1986, Rudashevsky 1989). The solid solutions form isolated grains 30–75 μm to 250 μm in size. Note that they are distributed in the high-temperature isoferroplatinum only exceptionally.

The crystallization of PGM at the magmatic stage is limited to isoferroplatinum and solid solutions in the system Os–Ir–Ru–Pt. The postmagmatic stage of evolution is characterized by a much greater variety of mineral species.

Tetraferroplatinum, tulameenite and hongshiite

Platinum-dominant solid solutions are tetraferroplatinum, tulameenite, and hongshiite. They are rare in the Konder massif and most commonly form a rim of variable thickness on isoferroplatinum, but may completely replace it. Tetraferroplatinum exhibits the most consistent composition, invariably containing Cu (up to 3 wt.%) and Ni (up to 1.5 wt.%). Tulameenite forms a rim on grains of isoferroplatinum; it contains variable Fe (8.5–13 wt.%) and Cu (8.8–12.8 wt.%), but constant Pt contents. In rare isolated segregations of tulameenite associated with bornite, irregularly distributed impurities of Ni (up to 3.5 wt.%) and Ir (up to 2.5 wt.%) occur, showing an enrichment as the rim is approached. Variants of tulameenite enriched in Sn and Sb also are found (Rudashevsky *et al.* 1992). Even within the same rim around isoferroplatinum, the tulameenite is represented by both marginal and intermediate members of the solid-solution series Pt(Fe,Cu)–Pd(Cu,Fe). Hongshiite seems to be the most variable in composition (Table 3).

PGE sulfides and sulfoarsenides

PGE sulfides and sulfoarsenides are much more widespread at the postmagmatic stage in the Konder massif. Members of the laurite–erlichmanite series and sulfoarsenides of the irarsite–hollingworthite series are the most common. Monosulfides and compound sulfides of malanite – cuprorhodsite – cuproiridsite composition are less common. Sulfides such as inaglyite and konderite are much rarer. All these compounds form a fragmentary rim (10 μm wide or more) or lens-like and equidimensional segregations (5–75 μm) at grain boundaries and at the margins of isoferroplatinum grains.

PGE monosulfides are represented by cooperite and a nickel-rich variety of a pentlandite-like phase. Electron-microprobe analyses show that cooperite has a composition close to PtS. Its block-shaped and needle-shaped segregations form a rim around grains or veinlets of isoferroplatinum in tulameenite in some instances. However, the bulk of the cooperite is related to concentrations of pentlandite, chalcocite, bornite, chalcopyrite, and cubanite that form rare lenses and veinlets in dunite

in the southwestern part of the Konder massif (Emel'yanenko *et al.* 1989).

Pentlandite-like monosulfides have been found intergrown with magnetite and pyrrhotite in dikes of magnetite–phlogopite pyroxenite. In the last case, the PGE (Ir mainly) account for only 26 wt.% of the monosulfide fraction (Table 4). This material is isotropic, and has a microhardness in the range 180–220 kg/mm². Analogues of pentlandite-type phases described earlier are enriched in Ir and Rh, or rarely only in Rh, or in a single case, Rh and Ru. Along with Fe and Ni, it contains Co and Cu (up to 2.5 and 5.8 wt.%) also (Cabri *et al.* 1981, Evstigneeva *et al.* 1992).

TABLE 3. CHEMICAL COMPOSITION OF HONGSHIITE AND ITS Pd-DOMINANT ANALOGUE, KONDER ALKALI-ULTRABASIC MASSIF, RUSSIA

No.	Pt	Pd	Cu	Fe	Ag	Total
1	25.20	40.97	26.16	5.23	0.42	97.98
2	25.65	41.02	26.41	5.20	0.26	98.54
3	67.33	8.62	15.06	7.97	-	98.98
4	71.42	5.91	13.68	8.80	-	99.81
5	67.58	7.98	15.63	8.21	-	99.40
6	58.73	14.68	19.04	7.53	-	99.98
7	48.78	21.75	20.81	6.78	0.19	98.31
8	20.32	45.83	28.44	5.06	0.38	100.03

Compositions are expressed in wt.%.

TABLE 4. COMPOSITION OF MONOSULFIDE OF THE PGE AND IRON-GROUP ELEMENTS, KONDER ALKALI-ULTRABASIC MASSIF

No.	Pt	Ir	Rh	Fe	Ni	Cu	S	Total
1	2.13	26.23	2.21	19.21	17.93	2.88	27.66	98.24
2	1.09	25.54	2.71	19.96	18.31	2.87	28.29	98.77

Compositions are quoted in wt.%.

TABLE 5. CHEMICAL COMPOSITION OF PGE THIOSPINELS, KONDER ALKALI-ULTRABASIC MASSIF, RUSSIA

No.	Cu	Fe	Pt	Ir	Rh	S	Total
1	8.18	1.38	11.34	49.08	3.08	24.08	97.14
2	5.04	1.15	13.63	33.76	14.59	23.74	99.82
3	9.94	1.70	30.27	26.60	7.97	23.59	101.06
4	8.83	3.41	17.98	25.54	17.77	25.13	98.66
5	10.56	0.51	25.19	24.04	13.62	26.35	100.27
6	10.64	0.77	33.42	20.38	9.11	25.32	99.64
7	11.69	-	38.11	17.36	6.76	25.47	99.39
8	8.28	1.77	30.27	6.21	21.45	26.63	100.98

Note: additional determinations have been included in the totals: Os in compositions 2, 3 and 8 (5.11, 0.52, 4.39%), Pd in compositions 2, 3 and 8 (2.33, 0.47, 1.98%), and Ni in composition 2 (0.47 wt.%).

Compound sulfides, represented largely by a thiospinel of the malanite – cuprorhodite – cuproiridsite group and, rarely, by a Cu- and Pb-bearing mineral of the inaglyite – konderite group (Rudashevsky *et al.* 1984a, b, 1985), form equidimensional inclusions and veinlet-like grains of isoferroplatinum and a thin rim around them. Individual rounded grains, up to 0.3 mm in size, and polymineralic intergrowths with iridosmine, erlichmanite, laurite and, in some cases, with sperryite, bismutharsenide, irarsite, and hollingworthite, are much rarer. These minerals occur predominantly in the same samples of dunite in which lenses and veinlets of Cu, Fe, Ni sulfides with Co, Pt impurity up to 0.8 wt.% Co, 2.5 wt.% Pt were found.

The maximum Pt, Ir, and Rh content in the thiospinel is 38, 49 and 21 wt.%, respectively (Table 5). Most grains of thiospinel correspond to malanite with a high concentration of Rh and Ir, but others are cuproiridsite, the rhodium analogue, iridian cuprorhodite, and an essentially platinum-rich variety of the cuprorhodite (Fig. 4). Fe (up to 3.4 wt.%) is invariably present in these thiospinels.

Among the Cu- and Pb-bearing sulfides we have studied (Table 6), inaglyite saturated with rhodium is the most prevalent. One of these sulfides is konderite, with much less iridium than that described earlier (Rudashevsky *et al.* 1984a), and the other two varieties are enriched in the Cu₃PbPt₈S₁₆ end-member (up to 46%) and represent a new mineral, the Pt-dominant analogue of inaglyite and konderite (Fig. 5). Like the other two minerals, this sulfide has a microhardness of 412–435 kg/mm² and contains little Fe, and no Ni; however, we established the essential impurity as As (up to 3.96 wt.%).

In the Konder River placer, we have found a complex sulfide that contains palladium and gold (in wt.%: 52.47 Pd, 11.53 Au, 4.94 Ag, 15.64 Bi, 8.46 Pb, 0.69 Ni, 7.34 S, total: 101.07) with the general formula (Pd,Au,Ag,Ni)₁₁(Bi,Pb)₂S₄. Together with palladium germanide (Pd₂Ge), discovered probably for the first time, it forms a heterogeneous rim of variable composition around grains of hongshiite. Experimental investi-

TABLE 6. CHEMICAL COMPOSITION OF Cu- AND Pb-BEARING SULFIDES OF THE PGE, KONDER ALKALI-ULTRABASIC MASSIF

No.	Pb	Cu	Ir	Pt	Rh	S	Total
1	8.12	9.32	18.73	29.15	9.25	24.12	99.43
2	7.60	10.12	18.20	30.67	9.14	24.47	100.92
3	8.84	7.96	24.32	21.54	12.56	24.43	99.65
4	8.43	9.32	23.45	22.31	11.73	24.17	99.41
5	8.18	8.92	20.12	16.58	18.70	25.12	100.40
6	7.44	7.92	26.15	19.72	11.05	24.17	100.41
7	8.07	8.16	26.32	19.84	11.34	23.91	99.87

Note: additional determinations have been included in the totals: Fe in compositions 1 and 2 (0.74, 0.72%) and As in compositions 5–7 (2.78, 3.96 and 2.23 wt.%).

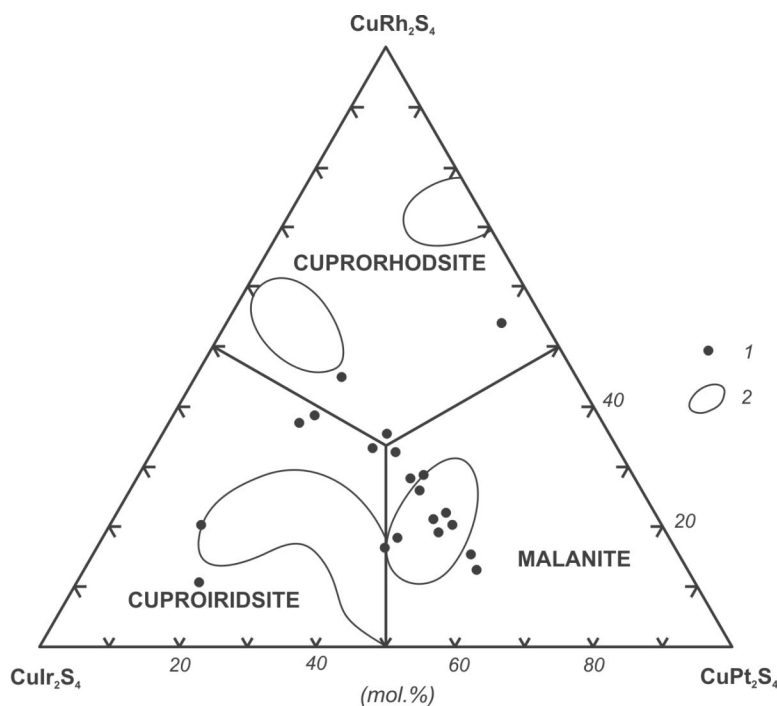


FIG. 4. Compositions of PGE thiospinels. 1) PGE thiospinel of Konder massif according to our data (Table 5); 2) fields of PGE thiospinel compositions (after Rudashevsky *et al.* 1985).

gations of the systems Au–Ag–S and Au–Bi–S (Nekrasov 1991) show that the gold-bearing sulfide could have originated only at relatively low temperature (200–350°C) and extremely high $f(S_2)$ (10^{-2} – 10^{-3} Pa).

Disulfides of the erlichmanite–laurite series are represented by both end members and less common examples of intermediate compositions (Fig. 6). Zoned grains are the general case, with osmian laurite and ruthenian erlichmanite both enriched in Ru near the rim compared with the center. These minerals contain a variable level of Pt (0.2–2.1), Rh (0.5–5.1), Ir (0.2–9.9), Pd (0.5–2.7), and As (0.4–2.2 wt.%). Analogous disulfides of Pt and Rh have been noted in alpine-type ultrabasic massifs (Dmitrenko *et al.* 1985). However, the latter contain less Pd and commonly more Ir.

A sulfarsenide of the irarsite–hollingworthite series is as common as Os–Ru disulfides and formed almost simultaneously with these, on the basis of observations of interrelations in polymineralic grains.

Like the disulfides, the sulfarsenides are represented by both the end members and intermediate compositions, which is not typical of PGM occurrences related to alpine-type ultrabasic massifs (Fig. 7). Along with isolated homogeneous inclusions of irarsite and hollingworthite, their zonally arranged segregations, in

which the marginal part is enriched in Ir and the center in Rh, are commonly found in isoferroplatinum. Much more complicated formations, with a zonal structure (50–200 μm in size) also are present. Their core is composed of iridosmine, which gives way to irarsite enriched in osmium toward the periphery, and then to hollingworthite, forming a narrow (5–8 μm) rim. Platarsite occurs as isolated grains (Mochalov 1986, Rudashevsky *et al.* 1992).

The content of Pt, Os, and Ru impurities in the Konder irarsite–hollingworthite sulfarsenides varies less widely (0.2–4.6 wt.%) than in their analogues from alpine-type ultrabasic rock, in which the maximum concentrations of these PGE are twice as large (Dmitrenko *et al.* 1985), except for Pd, which seems saturated (0.4–4.8 wt.%).

Sperrylite and Pt₂As₃

PGE arsenides are represented mainly by sperrylite. The compound Pt₂As₃, first found here, and complex Sb-, Bi-, and Te-bearing Pd and Pt arsenides are rare. Sperrylite occurs as fine (50–250 μm) inclusions in isoferroplatinum and composite grains with tulameenite. Single octahedra up to 1.5 mm across are much rarer.

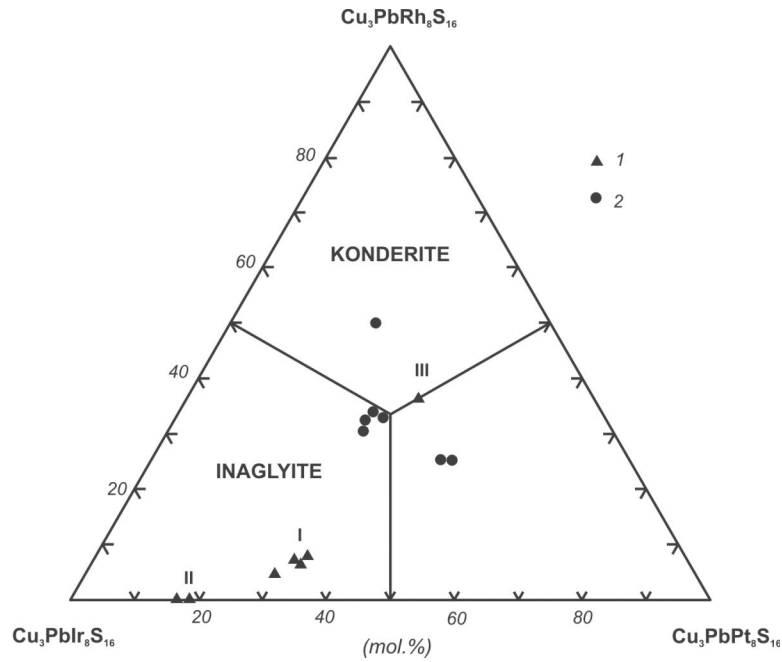


FIG. 5. Compositions of Cu–Pb-bearing sulfides of PGE. 1) Inaglyite (I, II) and konderite (III) from Inaglinsky (I), Nizhne–Tagilsky (II) and Konder (III) massifs (after Rudashevsky *et al.* 1984a, b); 2) inaglyite, konderite, and what is likely to be a new platinum analogue (Table 6).

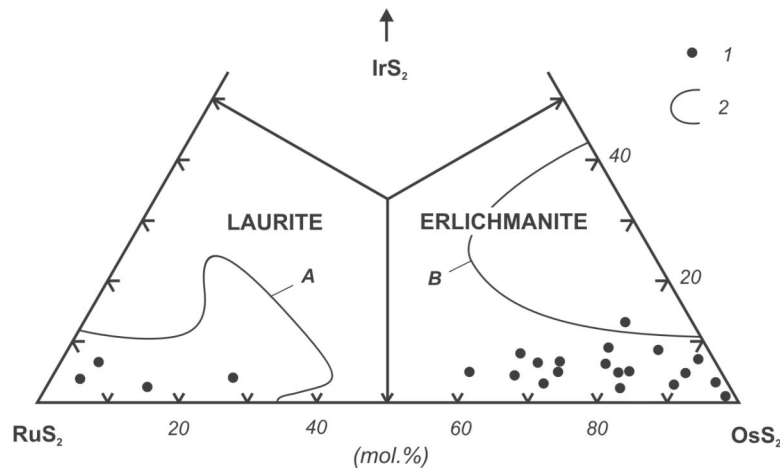


FIG. 6. Compositions of PGE disulfide of the erlichmanite–laurite series. 1) PGE disulfides of Konder massif according to our data (after Nekrasov *et al.* 1994); 2) fields of mineral compositions of laurite (A) – erlichmanite (B) series from alpine-type ultrabasic rocks (after Dmitrenko *et al.* 1985).

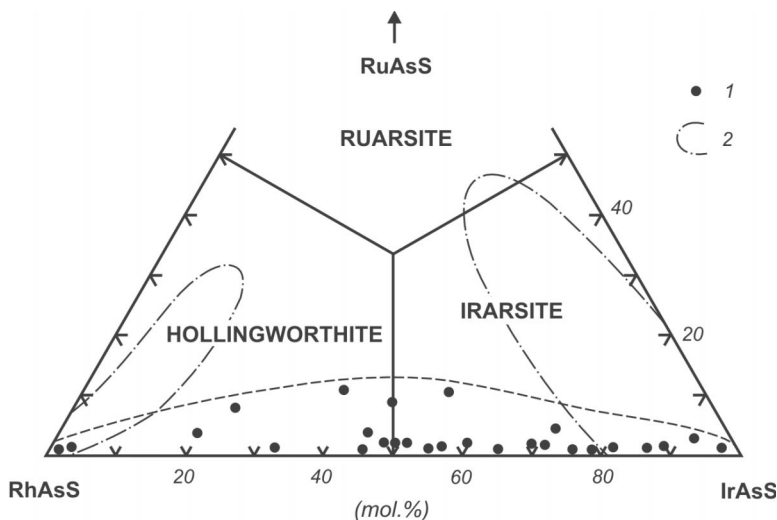


FIG. 7. Compositions of sulfoarsenide of Rh–Ir–Ru system of Konder massif. 1) PGE sulfarsenides of the Konder massif according to our data (after Nekrasov *et al.* 1994); 2) fields of sulfarsenide compositions from alpine-type ultrabasic rocks (after Dmitrenko *et al.* 1985).

The association of sperrylite with antimonpalladinite, irarsite, and cooperite has been also encountered. The chemical composition of sperrylite is close to being stoichiometric PtAs_2 , with a negligible proportion of sulfur in most samples; this finding does not contradict the experimental data of Makovicky *et al.* (1990), according to which the solubility of S in PtAs_2 at 850° and 470°C attains 2.5 wt.%. In their experiments, sulfur-bearing sperrylite precipitated in association with cooperite, pyrrhotite, and platarsite, which may be an indication of high $f(\text{S}_2)$ in the natural ore-forming system. Although the associations of sperrylite are diverse within the system Fe–Pt–As–S, these experiments showed that PtAs_2 is the only stable binary phase. In other words, we did not expect to find the fine inclusions of the compound $\text{Pt}_{1.5}\text{Ir}_{0.5}\text{As}_3$ (in wt.%: 51.62 Pt, 1.08 Rh, 10.57 Ir, 0.28 Os, 0.16 Cu, 2.2 S, 33.14 As, total: 99.05; approximately 25 μm , microhardness 500 kg/mm²) with a calculated formula $(\text{Pt}_{1.57}\text{Ir}_{0.33}\text{Rh}_{0.06})_{\Sigma 1.96}(\text{As}_{2.63}\text{S}_{0.40})_{\Sigma 3.03}$ (Fig. 8) in isoferroplatinum. A close analogue of this mineral is a phase enriched in Rh and S with the formula $(\text{Pt,Rh})_2(\text{As,S})_3$, discovered in a gold–platinum placer in Russia (Shcheka *et al.* 1991). In this connection, it seems that the presence of Ir (up to 10.6 wt.%) or Rh (up to 6.2 wt.%) as impurities in the Pt_2As_3 compound must stabilize its structure.

Composite palladium and platinum arsenides

In composite palladium and platinum arsenides (Table 7), in spite of considerable variations in the con-

TABLE 7. CHEMICAL COMPOSITION OF COMPOSITE Sb-, Bi-, AND Te-BEARING ARSENIDES OF PALLADIUM AND PLATINUM, KONDER ALKALI-ULTRABASIC MASSIF, RUSSIA

No.	Pd	Pt	Ag	Sb	Bi	Te	As	Total
1	61.63	15.67	1.30	13.95	-	0.43	7.80	100.78
2	73.03	1.32	2.38	12.46	1.68	0.32	7.60	98.79
3	70.27	1.12	2.59	19.59	0.55	-	5.54	99.66
4	69.63	0.40	0.84	23.26	-	-	2.28	99.25
5	67.61	-	0.72	15.95	-	0.12	9.44	98.00
6	69.87	-	-	25.51	-	-	3.01	100.01
7	64.94	2.10	1.05	3.75	17.58	1.46	6.64	98.35
8	65.67	1.11	0.62	0.66	22.38	1.89	6.20	99.81
9	66.87	0.94	1.05	2.65	16.88	1.95	6.06	99.02
10	63.69	12.43	0.65	-	13.87	-	9.49	100.13
11	64.48	11.78	0.54	-	13.56	-	9.26	99.62
12	72.11	4.45	0.16	0.42	9.46	6.13	4.74	97.47
13	72.76	3.18	0.31	1.87	7.01	6.94	5.33	97.40

Note: additional determinations have been included in the totals: Sn in compositions 4 (1.43%) and 9 (0.19%), Cu in compositions 4 (1.41%), 5 (4.16%) and 6 (1.62%), and Pb in compositions 7 (0.83%), 8 (1.28%) and 9 (2.43 wt.%). 1–6: antimonarsenides, 7–11: bismutharsenides, 12–13: bismuthotellurarsenides.

tent of all components, the ratio of Pd (or Pd + Pt + Ag) to $\Sigma(\text{As, Bi, and Sb})$ in most of minerals approximates 3:1, as in the discredited species “guanglinitite”, and correspond to the generalized formula $(\text{Pd,Pt})_3(\text{Bi,Sb,Te,As})$. Among these, the antimony and bismuth arsenides predominate. The exceptions are two antimony arsenides (Table 7, anal. 1, 2), two bismuth arsenides (anal. 10, 11), and both bismuth tellurarsenides. One of the antimony arsenides (anal. 1) exhibits the isomertiteite

formula, $(\text{Pd}_{9.66}\text{Pt}_{1.34})_{\Sigma 11}(\text{Sb}_{2.18}\text{As}_{1.73}\text{Te}_{0.05})_{\Sigma 3.96}$. The other antimony arsenide is similar to the previous case; however, its inferred chemical composition gave a somewhat different formula, $(\text{Pd}_{9.59}\text{Pt}_{0.10}\text{Ag}_{0.31})_{\Sigma 10}(\text{Sb}_{1.43}\text{As}_{1.41}\text{Bi}_{0.11}\text{Te}_{0.04})_{\Sigma 2.99}$. One of the bismuth tellurarsenides seems to be similar to "guanglinit" and has an inferred formula $(\text{Pd}_{3.89}\text{Pt}_{0.09}\text{Ag}_{0.02})_{\Sigma 4}(\text{Bi}_{0.16}\text{Sb}_{0.09}\text{Te}_{0.31}\text{As}_{0.40})_{\Sigma 0.96}$. The other bismuth arsenide ranges in composition (Table 7) and cation : anion ratio from 7:2 (anal. 10, 11) to 9:2 (anal. 12), and is similar to arsenopalladinite (Fleischer & Mandarino 1995), and more precisely to its Bi-bearing (anal. 10, 11) and Bi-Te-bearing (anal. 12) variants. Most of the composite Pd and Pt arsenides are found in the form of fine isolated inclusions in isoferroplatinum, the palladium-dominant analogue of hongshiite, and palladium-, copper-bearing gold, where they usually are associated with sobolevskite and other bismuthides and antimony bismuthides of palladium, which form in some cases polymineralic aggregates up to 90 μm in size. The associations with sperrylite are rarer.

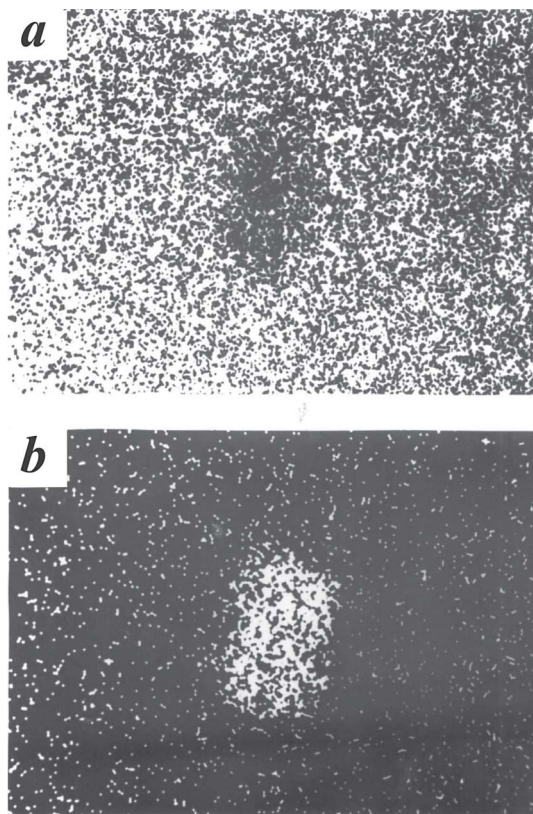


FIG. 8. X-ray maps of the isoferroplatinum grain enclosing a new platinum arsenide (1200 \times); a) $\text{PtL}\alpha$, b) $\text{AsK}\alpha$.

Bismuthides, antimonbismuthides, antimonides and tellurides

Bismuthides, antimonbismuthides, and antimonides of palladium, represented by minerals of sobolevskite (PdBi) – sudburyite (PdSb) series, are rare at Konder. Fine inclusions (10–25 μm) of sobolevskite close to the stoichiometry PdBi (Table 8) are common in copper-bearing gold, and rarer in isoferroplatinum. Many bismuthide grains are zoned. The central part is composed of PdBi, whereas the margin is enriched in palladium, up to a composition corresponding to the stoichiometry Pd_5Bi_2 and Pd_3Bi . We found both as individual phases and in a grain of tetra-auricupride containing 8.69 wt.% Pt and 0.36 wt.% Pd, and as rare inclusions in froodite, PdBi_2 (Table 8). As long as Sb is available to replace Bi in sobolevskite, sudburyite eventually forms. Several small grains of this mineral (Table 8), up to 25 μm in size, were found in composite grains with sobolevskite and the phase $\text{Pd}_3(\text{Bi,Sb})$, enclosed in gold. In some cases, needle-shaped inclusions of native antimony are present in the gold. Antimonides, arsenide–antimonides, sulfantimonides, and phases of more complex composition, with the ratio of the PGE to the "anion" portion from 5:2 and 3:1 to 1:2, also were found closely intergrown with bismuthides of the sobolevskite–sudburyite series. Rhodium–iridium sulfantimonide, $(\text{Rh,Ir})\text{SbS}$, similar to tolovkite (ideally, IrSbS) was first discovered at Konder by Mochalov (1986). Later, a similar mineral was discovered by Evstigneeva *et al.* (1992) at Yubdo, Ethiopia. Many grains of these minerals are zoned.

Minerals of sobolevskite (PdBi) – kotulskite (PdTe) series have a limited distribution. Owing to the complete solid-solution between Te and Bi, even within the

TABLE 8. CHEMICAL COMPOSITION OF BISMUTHIDES AND ANTIMONBISMUTHIDES OF PALLADIUM AND PLATINUM, KONDER ALKALI-ULTRABASIC MASSIF, RUSSIA

No.	Mineral and its generalized formula	Pd	Pt	Sb	Bi	Total
1	Sobolevskite, PdBi	31.83	-	-	69.94	101.77
2	<i>ibid.</i>	31.33	-	-	70.58	101.91
3	<i>ibid.</i>	31.35	-	-	64.88	99.02
4	<i>ibid.</i>	23.69	9.82	-	64.98	99.77
5	Pd_5Bi_2^*	57.69	-	-	43.68	101.37
6	"Bismuthpalladinite", Pd_3Bi_2^*	44.27	-	-	55.31	99.58
7	<i>ibid.</i>	47.27	-	-	52.00	99.27
8	$\text{Pd}_3(\text{Bi,Sb})^*$	77.26	-	15.01	8.14	100.41
9	<i>ibid.</i>	77.34	-	15.03	8.54	100.91
10	$(\text{Pt,Pd})(\text{Bi,Sb})^*$	12.23	34.10	13.64	39.95	99.92
11	Froodite, PdBi_2	19.76	8.80	3.60	64.94	100.59
12	Sudburyite, $\text{Pd}(\text{Sb,Bi})$	42.25	-	42.43	14.34	99.02
13	<i>ibid.</i>	41.34	-	41.08	16.16	98.58
14	Insizwaite, PtBi_2	-	31.39	3.57	66.09	101.05

Note: additional determinations have been included in the totals: Cu in compositions 3 (0.52%) and 11 (3.49%), Au in compositions 3 (2.27%) and 4 (1.28 wt.%). Minerals that probably are new species are shown by an asterisk.

same host-mineral (tetra-auricupride or isoferroplatinum), inclusions of two or three phases may be present. These phases differ from one another in composition, as a result of complete substitution involving Te and Bi, and are intermediate compounds between sobolevskite and kotulskite (Table 9). In some of them, the impurity elements are Pb (to 2 wt.%) and Pt (to 2.7 wt.%). Members of the series kotulskite (PdTe) – sudburyite (PdSb) contain a bismuth-free phase with a high concentration of Sb (more than 15 wt.%), which may be a new mineral (Table 9).

The Bi–Te-bearing palladinite that we found is a much more widespread mineral than the members of the sobolevskite–kotulskite solid solution (Table 9). It occurs as fine inclusions (10–15 μm) in bornite from the sulfide lenses in the Konder dunite, mentioned above, and in low-grade gold. This mineral is characterized by striking heterogeneities, with small-scale variations of 2–3 wt.% Pd and 0.5–1.5 wt.% in other elements. Some Bi–Te-enriched domains of palladinite have decomposed into two or three phases, one of which is Pt oxide and other two are identified as Bi_3Te and native bismuth. The Bi_3Te compound occurs also as individual mica-like accumulations up to 5 μm across. In aggregates with high-grade Au (fineness 880–920), the Bi_3Te precipitated later and cemented segregations of gold.

Insizwaite, PtBi_2 , occurs in isoferroplatinum (Table 8), earlier first described at Konder by Mochalov (1986), and in geversite, $\text{Pt}(\text{Sb},\text{Bi})_2$, as discovered by Rudashevsky *et al.* (1992); it is not common in the Konder massif. A palladium bismuth plumbide is present as single grains. We found it in copper-bearing gold as inclusions 5–15 μm in size. The chemical composition of this presumably new phase (wt.%) is: 57.52 Pd, 34.74 Pb, 7.02 Bi, 1.2 Pt, total 100.48. Rare inclusions of zvyagintsevite are present in tetra-auricupride.

Platinum and palladium stannides

Platinum and palladium stannides are relatively widespread, in the form of fine (15–60 μm) inclusions in tetra-auricupride, tulameenite, and isoferroplatinum. Their chemical composition (Table 10) allows us to

subdivide them into three groups. The first one (Table 10, anal. 1 and 2) has a negligible level of Sb (up to 1 wt.%) and is free of Cu. The sum of Pt and Pd is 82 wt.%, with about 17 wt.% Sn, and the composition as a whole was calculated on the basis of the formula of rustenburgite, $(\text{Pt},\text{Pd})_3\text{Sn}$. The second group includes the multicomponent copper-enriched (up to 14 wt.%) alloys of the system Pt–Pd–Sn–Cu–Fe (Table 10, anal. 3 to 9). Impurities are Ni (up to 0.4 wt.%) and Bi (up to 1.3 wt.%). The compounds of this group are characterized by notable variations in Sn content (9–17.2 wt.%), relatively constant Pt (63–73.4 wt.%), and the almost invariant presence of Fe (up to 5.8 wt.%). These phases are associated with sobolevskite and palladium-bearing gold. High-palladium solid solutions, which have been described already from the Konder massif (Mochalov 1986), represent the third group of stannides.

Palladium germanide

As was noted above, we found palladium germanide (Pd_2Ge) in the Konder massif. It is a new, as yet unnamed mineral, which together with a new palladium–gold-bearing sulfide, make a narrow (5–17 μm) rim around a grain of the palladium analogue (PdCu) of hongshiite (Fig. 9). Although high magnification reveals an optical heterogeneity, consisting of a rhythmic alternation of fine strips of the germanide, all eight analyses of the same grain show similar results, that on average are described by the composition (wt.%): 75.62 Pd, 1.12 Ag, 23.89 Ge, total: 100.63. The experiment carried out by I.Ya. Nekrasov (unpubl. data) at dry conditions at 700°C shows that in the system Ge–Pd, along with Pd_2Ge , three other phases, PdGe , Pd_4Ge , and Pd_5Ge , are stable, which allow us to anticipate their existence in nature.

PGE oxide and hydroxide

PGE oxide and hydroxide compounds formed at the final stage (Augé & Legendre 1992, Evstigneeva *et al.*

TABLE 9. CHEMICAL COMPOSITION OF BISMUTHOTELLURIDES AND ANTIMONTELLURIDES OF PALLADIUM, KONDER ALKALI-ULTRABASIC MASSIF, RUSSIA

No.	Pd	Ag	Sb	Bi	Te	Total
1	44.24	-	-	13.62	38.19	97.99
2	44.72	0.19	-	12.39	39.45	98.87
3	42.42	0.57	15.64	-	38.81	98.31
4	32.42	-	-	55.17	11.34	101.62
5	69.92	0.94	0.35	9.14	16.69	97.04

Note: additional determinations have been included in the totals: Pb in compositions 1 (1.94%), 2 (2.12%) and 3 (0.87%), and Pt in composition 4 (2.69 wt.%).

TABLE 10. CHEMICAL COMPOSITION OF PLATINUM AND PALLADIUM STANNIDES, KONDER ALKALI-ULTRABASIC MASSIF, RUSSIA

No.	Pt	Pd	Cu	Sn	Sb	Fe	Total
1	66.12	15.40	-	16.90	0.66	-	99.08
2	62.84	17.68	-	16.96	1.07	-	98.55
3	63.02	5.00	14.05	16.64	-	0.18	99.83
4	68.12	3.18	13.09	13.82	-	1.75	99.96
5	63.48	4.69	13.50	16.27	-	0.36	99.59
6	72.49	0.34	12.16	9.01	-	5.78	99.78
7	63.41	5.32	13.75	17.18	-	-	99.66
8	72.66	-	12.51	10.75	0.36	3.30	99.98
9	73.44	-	12.95	10.28	0.35	2.52	99.54

Note: additional determinations have been included in the totals: Bi in compositions 3, 5 (0.94, 1.29 wt.%) and Ni in composition 8 (0.4 wt.%).

1992, Nekrasov *et al.* 1994). They are the products of supergene events in most cases; however, they may also be hypogene, in part as a result of interaction of PGM of an early (magmatic) stage with postmagmatic solutions.

In most cases, oxides and hydroxides developed at the expense of isoferroplatinum, tulameenite, and hongshiite. In addition to Pt(Pd), they preserve the high Fe and Cu contents. Palladium, Os, Rh, and Ir oxides are much rarer in the Konder placer (Table 11). For example, Pd oxide coats the palladium analogue of hongshiite, Pd(Cu,Fe), as a thin film, but Pt, Ir, Os, and Rh oxides result from the partial replacement of hongshiite, minerals of irarsite–hollingworthite series

and other PGM. The analytical totals in the case of the hydroxides vary over the range 70–80 wt.% (Table 12), depending on the amount of H₂O in the structure (Mochalov 1986, Nekrasov *et al.* 1994).

Gold mineralization

The gold mineralization in the Konder massif is extremely diverse. Numerous electron-microprobe results indicate not only native and Ag-bearing gold, but also Cu-, Cu–Pd-, and Cu–Pt-enriched varieties (Nekrasov *et al.* 1994, 2001), which are exceptionally rare in nature (Novgorodova 1983, 1994).

The gold minerals formed later than the cubes of platinum and, probably, somewhat later than the PGE sulfides and sulfoarsenides, but contemporaneously with various Pd-bearing compounds including hongshiite and its Pd-dominant analogue, complex sulfides, arsenides, antimonides, bismuthides, tellurides, stannides, plumbides, and palladium germanide.

The compounds of gold and other metals can be divided into three broad groups (Fig. 10), distinguished by proportions of Au, Cu, Ag, Pd, and Pt (Nekrasov *et al.* 2001). The first group of solid solutions comprises the compounds based on Au and Cu, belonging to the systems Au–Cu, Au–Cu–(Pd,Pt), and Au–Cu–Ag. They form fine tabular and spindle-shaped inclusions in Ag-

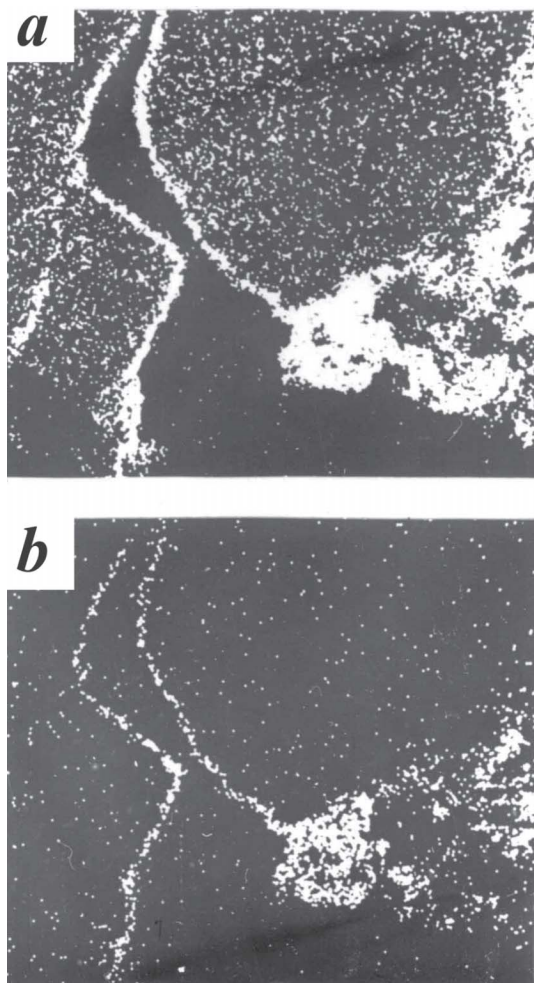


FIG. 9. X-ray maps of edge part of the Pd-bearing hongshiite grain in contact with palladium germanide, which forms heterogeneous units continuous into a rim (1000×); a) PdL α , b) GeL α .

TABLE 11. CHEMICAL COMPOSITION OF PGE OXIDES, KONDER ALKALI-ULTRABASIC MASSIF, RUSSIA

No.	Pt	Pd	Ir	Os	Rh	Cu	Fe	Total
1	3.76	54.1	-	-	-	22.43	7.93	88.22
2	65.86	-	-	-	-	13.61	5.89	85.36
3	81.18	-	-	-	-	1.54	6.94	89.66
4	64.09	-	-	-	-	15.20	4.44	83.73
5	63.51	-	-	-	-	19.64	6.63	83.78
6	66.96	-	-	-	-	9.91	11.99	88.86
7	77.74	-	-	-	-	-	6.93	86.72
8	74.08	-	-	-	-	-	6.08	84.54
9	-	-	21.28	51.16	0.14	-	3.31	83.94
10	3.68	-	34.72	1.27	31.26	2.02	12.03	84.98

Note: additional determinations have been included in the totals: Ru in composition 9 (8.05 wt.%) and Au in compositions 7 and 8 (2.05 and 4.38 wt.%).

TABLE 12. CHEMICAL COMPOSITION OF PGE HYDROXIDES, KONDER ALKALI-ULTRABASIC MASSIF, RUSSIA

No.	Pt	Pd	Ir	Os	Rh	Cu	Fe	Total
1	6.35	0.69	48.57	-	6.71	2.04	6.08	70.44
2	8.07	-	53.16	0.32	4.28	-	7.92	73.92
3	4.19	-	40.27	0.44	28.62	-	0.76	74.51
4	75.52	1.92	-	-	-	-	6.93	77.45
5	1.76	-	26.53	6.01	30.02	10.20	2.84	77.56

Note: additional determinations have been included in the totals: Ru in compositions 2, 3 (0.17, 0.23 wt.%) and Bi in composition 4 (0.31 wt.%).

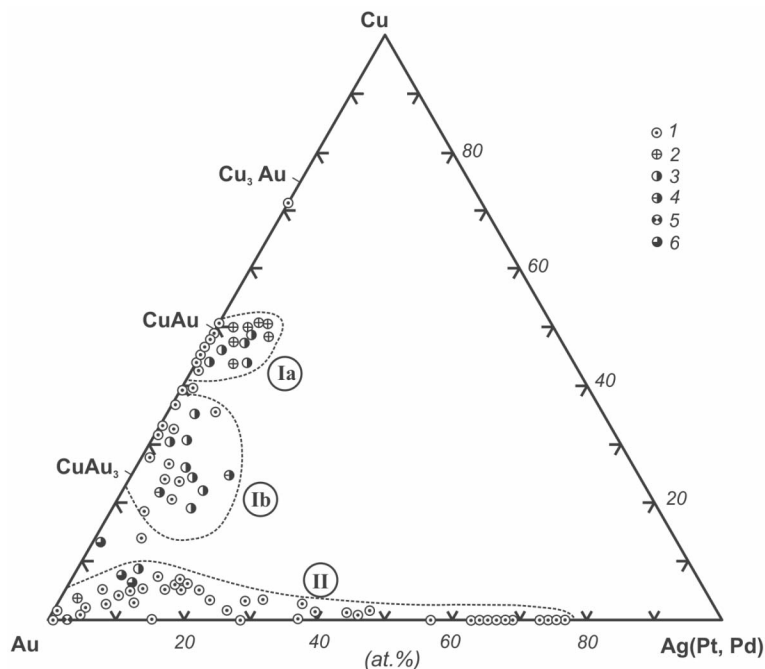


FIG. 10. Compositions of the gold solid-solution of Konder massif: Au-Cu, Au-Cu-Ag and Au-Ag (1), Au-Cu-Pt (2), Au-Cu-Pd (3), Au-Cu-Pt-Pd (4), Au-Cu-Pt with Ag (5), and Au-Cu-Pd with Ag (6). See text for other explanations.

bearing gold of high fineness, or serve as host minerals containing inclusions of Ag-bearing gold. In addition to forming discrete grains, both types of Cu-bearing and native gold intergrowths occur as zonal rims around the platinum crystals, and occasionally around other minerals. The Cu-bearing gold from Konder reveals a bimodal distribution of Cu (Fig. 10, I a, b) that demonstrates a high abundance of cupro-auride (Au_3Cu), which is lacking in other natural assemblages (Murzin *et al.* 1987, Novgorodova 1983, 1994, Sazonov *et al.* 1994), and tetra-auricupride (AuCu) with a whole range of Cu contents from 6.89 to 24.99 wt.% (Table 13). The Cu content, 44.27 wt.%, corresponding to auricupride (Cu_3Au), was detected in one sample only. Auricupride in association with tetra-auricupride is more typical of some other occurrences of Cu-bearing gold in the absence of cupro-auride (Novgorodova 1983). Some phases of Cu-bearing gold contain Ag (0.33–5.39 wt.%), which replaces Cu where Au content is no lower than 14 wt.%. The Pt and Pd in solid solution (0.22–11.79 wt.% and 0.18–10.27 wt.%, respectively) were established in a broader range of compositions within the Au-Cu series (8–25 wt.% Cu). Pt and Pd are present in various proportions, either separately or together (Table 14). The elevated Pt content is present only in AuCu, *i.e.*, in compositions enriched in Cu. The Cu-free Pd-bearing gold

(wt.%: 94.32 Au, 2.58 Pd) was detected at the margin of a complex grain of Pd-Cu-bearing gold with inclusions of zvyagintsevite ($(\text{Pd,Pt,Au})_3(\text{Sn,Pb})$).

The second broad group of natural Au compounds comprises its solid solutions with Ag (1.71–62.73 wt.%). This is mainly low-Cu (0.58–3.13 wt.%) native gold of moderate and high fineness (Table 15). The Au-Ag solid solutions richer in Ag also occur in heterogeneous grains (Fig. 10, II).

In the third broad group are the three-component compositions containing 3–5 wt.% Cu and 5–9 wt.% Ag. Where the concentration of these elements in gold is still higher, then the three-component alloy becomes unstable below 370–410°C (Nekrasov 1991) and breaks down into Au-Cu-(Ag) and Au-Ag-(Cu) phases. The proportions of phases in representative exsolution-induced intergrowths and the distribution of data points in the Ag-Cu-Au diagram show that the initial composition of the Au-Ag-Cu alloy that underwent exsolution during post-crystallization cooling was (at.%): from 51–55 to 72–75 Au, from 5–8 to 20–22 Ag, and from 12–14 to 32–35 Cu.

In addition to the close intergrowths of Cu- and Ag-bearing gold in heterogeneous grains and the gold dusting on platinum grains, gold of high fineness occurs as a film coating platinum nuggets in the Konder placers

(Nekrasov *et al.* 2001, Shcheka *et al.* 2004). Individual grains of gold with a high fineness (up to 990) at the margin and a lower fineness (750–820) in the core are sporadically found. The gold of high fineness was likely formed within the placer as a result of different solubility of Ag and Au in groundwater (Nekrasov *et al.* 1994). Gold grains with a high fineness in the core and low fineness at the margin are probably related to felsic rocks in the outer zones of the Konder massif.

CONCLUSIONS

A review of the PGM and gold encountered in the Konder alkaline-ultrabasic massif reveals an extremely diverse assemblage of accessory minerals related to the massif. This mineralization resembles the dispersed impregnations, predominantly of isoferroplatinum, in moderately chromium-enriched gabbro – pyroxenite – dunite intrusive bodies of the Urals and Alaska. At the same time, it resembles the manifestations of chalcogenides of PGE connected with the complex copper–nickel deposits in the layered intrusive bodies of basic rocks. Such a peculiarity of the Konder precious-metal

mineralization is caused by the existence of several stages of PGM formation at Konder, at magmatic and postmagmatic temperatures. For example, at the highest-temperature stage, mineralization occurred in low-chromite dunite of the core zone of the Konder intrusive complex; the crystallization of accessory isoferroplatinum enriched in minor PGE and of more unusual alloys in the system Ir–Os–Ru–Pt took place. Later, high-purity isoferroplatinum filled the interstices in lenses of massive chromite, chromite veins in dunites, and in dikes of magnetite clinopyroxenite. Formation of the more restricted but compositionally more widely variable chalcogenides of PGE occurred at the postmagmatic stage, with the participation of a residual fluid phase containing, along with platinum and palladium, Pb, Sn, Cu, Au, Ag, S, As, Bi, Sb, Te, and Ge. As a result of interaction of isoferroplatinum of the first stage of crystallization along its margin and along fractures with such a fluid phase, the PGE chalcogenides, tetraferroplatinum, tulameenite, hongshiite, as well as copper-bearing, platinum–copper-bearing, palladium–copper-bearing gold, and high-grade (fineness: more than 750) gold–silver solid solutions formed at the same time. The process of PGM formation at Konder ended with oxide and hydroxide compounds of supergene origin, mostly. Middle- and low-grade gold–silver solid solutions, found in placers, formed later than their high-grade analogues, and are related genetically with monzonite, which intruded the Konder ultrabasic suite.

TABLE 13. COMPOSITION OF Au–Cu SOLID SOLUTION, KONDER ALKALI-ULTRABASIC MASSIF, RUSSIA

No.	Au	Ag	Cu	Total	No.	Au	Ag	Cu	Total
1	75.03	-	24.42	99.45	7	86.55	0.34	11.37	98.26
2	79.05	-	21.50	100.55	8	86.64	-	14.34	100.98
3	78.14	-	21.92	100.06	9	86.20	0.55	13.56	100.31
4	76.38	-	23.75	100.13	10	89.15	2.84	7.44	99.43
5	76.29	-	23.02	99.31	11	86.12	3.27	9.47	98.86
6	83.99	-	16.12	100.11	12	55.50	-	44.27	99.77

Note: a portion of the 50 compositions available is given (Nekrasov *et al.* 2001). Compositions are given in wt.%.

TABLE 14. COMPOSITION OF Au–Cu–Pt AND Au–Cu–Pd SOLID SOLUTION, KONDER ALKALI-ULTRABASIC MASSIF, RUSSIA

No.	Au	Ag	Cu	Pt	Pd	Total
1	63.41	-	23.52	11.79	-	98.72
2	62.54	-	24.40	10.33	-	97.27
3	70.17	-	19.62	9.56	-	99.35
4	65.19	-	24.69	9.27	-	99.15
5	67.09	-	23.86	7.55	-	98.50
6	72.54	-	24.28	3.12	-	99.54
7	95.87	0.68	1.16	2.35	-	100.06
8	79.17	-	10.25	0.22	10.27	99.91
9	82.84	-	8.86	-	7.79	99.49
10	84.67	1.10	6.08	-	7.43	99.28
11	84.12	0.50	7.66	-	6.81	99.09
12	83.35	-	9.84	-	5.82	99.01
13	70.03	-	24.99	-	4.27	99.29
14	83.27	0.27	13.66	-	3.32	100.52

Note: a portion of the 23 compositions available is given (Nekrasov *et al.* 2001). Compositions are expressed in wt.%.

ACKNOWLEDGEMENTS

Drs. Louis J Cabri and Thierry Augé provided constructive criticism and many incisive comments, including language corrections; their help is greatly appreciated. Robert F Martin provided helpful comments, editorial serenity, support and encouragement. The authors are grateful to Galina G. Zubkova and Valentina A. Piskunova for help in computer processing of the manuscript and translation. We are also grateful to Sergey A. Shcheka for his critical review of the paper, and help in its revision.

TABLE 15. COMPOSITION OF Au–Ag ALLOYS, KONDER ALKALI-ULTRABASIC MASSIF, RUSSIA

No.	Au	Ag	Cu	Total	No.	Au	Ag	Cu	Total
1	98.31	1.09	0.46	99.86	8	81.48	17.14	1.56	100.18
2	97.86	1.71	0.71	100.28	9	75.70	23.46	-	99.16
3	94.82	2.84	1.92	99.58	10	69.71	29.83	0.11	99.65
4	89.68	7.11	3.02	99.81	11	69.97	30.29	0.12	100.38
5	88.89	8.70	2.09	99.68	12	59.30	41.13	-	100.43
6	86.23	14.08	-	100.31	13	50.35	47.96	-	98.31
7	84.79	12.31	2.01	99.11	14	45.78	53.21	-	98.99
					15	39.07	61.37	-	100.44

Note: a portion of the 39 compositions available (Nekrasov *et al.* 2001) is given. Compositions are expressed in wt.%.

REFERENCES

- ANDREEV, G.V. (1987): *The Konder Massif of Ultramafic and Alkaline Rocks*. Nauka, Novosibirsk, Russia (in Russ.).
- AUGÉ, T. & LEGENDRE, O. (1992): Pt-Fe nuggets from alluvial deposits in eastern Madagascar. *Can. Mineral.* **30**, 983-1004.
- BOGOMOLOV, M.A. (1964): Nature of crystalline schists and carbonate rocks near the Konder massif. In *Petrography of Metamorphic and Igneous Rocks of Aldan Shield*. Nauka, Moscow, Russia (32-56; in Russ.).
- CABRI, L.J., CRIDDLE, A.J., LAFLAMME, J.H.G., BEARNE, G.S. & HARRIS, D.C. (1981): Mineralogical study of complex Pt-Fe nuggets from Ethiopia. *Bull. Minéral.* **104**, 508-525.
- _____ & LAFLAMME, J.H.G. (1997): Platinum-group minerals from the Konder massif, Russian Far East. *Mineral. Rec.* **28**, 97-106.
- _____ & NALDRETT, A.J. (1984): Pattern of distribution and concentration of platinum-group elements in different geological settings. *27th Int. Geol. Congress, Mineralogy Reports* **10**. Nauka, Moscow, Russia (10-26; in Russ.).
- DMITRENKO, G.G., MOCHALOV, A.G., PALANDZHIAN, S.A. & GORYACHEVA, E.M. (1985): *Chemical Compositions of Rock-Forming and Accessory Minerals of Alpine-Type Ultramafic Rocks of Koryak Plateau. 2. Minerals of Platinum Elements*. USSR Acad. Sci., Far East Centre, North-Eastern Compound Research Inst., Magadan, Russia (in Russ.).
- EL'YNOV, A.A. & MORALEV, V.M. (1972): Massifs of ultramafic and alkaline rocks: depth of formation and erosion level. *Geol. Rudnykh Mestorozh.* **5**, 32-40 (in Russ.).
- EMEL'YANENKO, E.P., MASLOVSKY, A.N., ZALISHCHAK, B.L., KAMAIEVA, L.V. & FOMENKO, A.S. (1989): Regularities of the location of ore mineralization at the Konder alkaline-ultrabasic massif. In *Geological Conditions of the Localization of Endogenetic Ore Formation*. Far Eastern Branch, Academy of Sciences, Vladivostok, Russia (100-113; in Russ.).
- EVSTIGNEEVA, T.L., KUDRYAVCHEV, A.C. & RUDASHEVSKY, N.S. (1992): Platinum-group element minerals of Yubdo (Ethiopia): new data. *Mineral. Zh.* **14**, 29-41 (in Russ.).
- FLEISCHER, M. & MANDARINO, J.A. (1995): *Glossary of Mineral Species* (seventh ed.). The Mineralogical Record, Tucson, Arizona.
- HARRIS, D.C. & CABRI, L.J. (1991): Nomenclature of platinum-group-element alloys: review and revision. *Can. Mineral.* **29**, 231-237.
- LAPUTINA, I.P. (1980): Microprobe analysis of the platinum-group minerals. In *Electron-Probe Microanalysis in Mineralogy*. Int. Mineral. Assoc., Proc. XI Gen. Meeting. Nauka, Leningrad, Russia (42-52; in Russ.).
- LENNIKOV, A.M., OKTYABRSKY, R.A., SAPIN, V.I., TASKAEV, V.I., KISELEV, V.I. & DEMCHENKO, V.S. (1991): New data on rocks in metamorphic framework of the Konder massif. *Dokl. Akad. Nauk SSSR* **319**, 1187-1191 (in Russ.).
- MAKOVICKY, E., KARUP-MØLLER, S., MAKOVICKY, M. & ROSE-HANSEN, J. (1990): Experimental studies on the phase systems Fe-Ni-Pd-S and Fe-Pt-Pd-As-S applied to PGE deposits. *Mineral. Petrol.* **42**, 307-319.
- MARAKUSHEV, A.A., EMEL'YANENKO, E.P., NEKRASOV, I.YA., ZALISHCHAK, B.L. & MASLOVSKY, A.N. (1990): Formation of concentrically zoned structure of the Konder alkaline-ultramafic massif. *Dokl. Akad. Nauk SSSR* **311**, 167-170 (in Russ.).
- MOCHALOV, A.G. (1986): *Mineralogy of Platinum-Group Elements of Alpine-Type Ultramafic Rocks*. Dissertation, Department of Geological and Mineralogical Sciences, Leningrad State Univ., Leningrad, Russia (in Russ.).
- _____ (1994): Mineralogy of platinum-group elements from dunites. In *Geology, Petrology, and Ore Mineralization in the Konder Massif*. Nauka, Moscow, Russia (92-106; in Russ.).
- _____, ZHERNOVSKY, I.V. & DMITRENKO, G.G. (1988): Composition and distribution of native platinum and iron minerals in ultramafic rocks. *Geol. Rudnykh Mestorozh.* **5**, 47-58 (in Russ.).
- MURZIN, V.V., KUDRYAVTSEV, V.I., BERZON, R.O. & SUSTAVOV, S.G. (1987): The Cu-bearing ore in rodingite zones. *Geol. Rudnykh Mestorozh.* **5**, 96-99 (in Russ.).
- NEKRASOV, I.YA. (1991): *Geochemistry, Mineralogy, and Genesis of Gold Deposits*. Nauka, Moscow, Russia (in Russ.).
- _____, IVANOV, V.V., LENNIKOV, A.M., OKTYABRSKY, R.A., SAPIN, V.I. & TASKAEV, V.I. (1993): About specificity of solid solutions of system Os-Ir-Ru-Pt in alkaline-ultrabasic massifs. *Dokl. Akad. Nauk SSSR* **328**, 382-385 (in Russ.).
- _____, _____, _____, _____, _____, _____, ZALISHCHAK, B.L. & KHITROV, V.V. (1991a): New data on PGE mineralization of alkaline-ultrabasic concentrically zoned massifs of the Far East. *Dokl. Akad. Nauk SSSR* **320**, 705-709 (in Russ.).
- _____, _____, _____, _____, ZALISHCHAK, B.L., SAPIN, V.I. & TASKAEV, V.I. (1991b): Composition of Pt-Fe solid solutions as indicator of erosional level of platinum-bearing alkaline-ultrabasic ring intrusives. *Dokl. Akad. Nauk SSSR* **321**, 1049-1053 (in Russ.).
- _____, _____, _____, SAPIN, V.I., SAFRONOV, P.P. & OKTYABRSKY, R.A. (2001c): Rare natural polycomponent alloys based on gold and copper from a platinum placer in the Konder alkaline-ultrabasic massif, southeastern Aldan Shield, Russia. *Geol. Rudnykh Mestorozh.* **5**, 406-417 (in Russ.).

- _____, LENNIKOV, A.M., OKTYABRSKY, R.A., ZALISHCHAK, B.L. & SAPIN, V.I. (1994): *Petrology and Platinum Mineralization of the Alkaline-Ultrabasic Ring Complexes*. Nauka, Moscow, Russia (in Russ.).
- NOVGORODOVA, M.I. (1983): *Native Metals in Hydrothermal Ores*. Nauka, Moscow, Russia (in Russ.).
- _____. (1994): Crystal chemistry of native intermetallic compounds. *In Achievements of Science and Engineering, Seria Crystal Chemistry* **29** (in Russ.).
- OKTYABRSKY, R.A., SHCHEKA, S.A., LENNIKOV, A.M. & AFANAS'YEVA, T.V. (1992): The first occurrence of qandilite in Russia. *Mineral. Mag.* **56**, 385-389.
- ORLOVA, M.P. (1991): Geological structure and genesis of the Konder ultramafic massif. *Tikhookeanskaya geologia* **10**(1), 80-88 (in Russ.).
- PUSHKAREV, YU.D., KOSTOYNOV, A.I., ORLOVA, M.P., BOGOMOLOV, E.S. & GUSEVA, V.F. (2001): Sm-Nd, Rb-Sr, K-Ar and Re-Os isotopic constraints on the origin of PGE mineralization in the Konder massif, Khabarovsk region, Russia. *In Mineral Deposits at the Beginning of the 21st Century*. Swets and Zeitlinger Publ., Lisse, The Netherlands (677-680).
- RAZIN, L.V. (1976): Geologic and genetic features of forsterite dunites and their platinum-group mineralization. *Econ. Geol.* **71**, 1371-1376.
- RUDASHEVSKY, N.S. (1989): Evolution of chemical composition of osmium, ruthenium, and iridium hexagonal solid solutions in different formation of ultramafites. *Geologia i Geofizika* **10**, 68-74 (in Russ.).
- _____, BURAKOV, B.E., MALICH, K.N. & KHAETSKY, V.V. (1992): Accessory platinum mineralization of chomitites from Konder alkaline-ultrabasic massif. *Mineral. Zh.* **14**(15), 12-32 (in Russ.).
- _____ & MOCHALOV, A.G. (1985): Composition of chromian spinel inclusions into PGM grains from rocks of ultramafic formations. *Geologia i Geofizika* **8**, 56-69 (in Russ.).
- _____, _____, BEGIZOV, V.D., MEN'SHIKOV, YU.P. & SHUMSKAYA, N.I. (1984b): Inaglyite $\text{Cu}_3\text{Pb}(\text{Ir,Pt})_8\text{S}_{16}$ – a new mineral. *Zap. Vses. Mineral. Obshchest.* **113**, 712-717 (in Russ.).
- _____, _____, TRUBKIN, N.V., GORSHKOV, A.M., MEN'SHIKOV, YU.P. & SHUMSKAYA, N.I. (1984a): Konderite $\text{Cu}_3\text{Pb}(\text{Rh,Pt,Ir})_8\text{S}_{16}$ – a new mineral. *Zap. Vses. Mineral. Obshchest.* **113**, 703-711 (in Russ.).
- _____, MEN'SHIKOV, YU.P., MOCHALOV, A.G., TRUBKIN, N.V., SHUMSKAYA, N.I. & ZHDANOV, V.V. (1985): Cuprorhodsite CuRh_2S_4 and cuproiridsite CuIr_2S_4 – new natural thiospinels of platinum-group elements. *Zap. Vses. Mineral. Obshchest.* **114**, 187-195 (in Russ.).
- _____, _____, _____, _____, _____, MOCHALOV, A.G. & ORLOVA, M.P. (1982): Inclusions of silicates in natural iron-platinum alloys of the Konder massif. *Dokl. Akad. Nauk SSSR* **266**, 977-981 (in Russ.).
- SAZONOV, A.M., ROMANOVSKY, A.E., GRINEV, O.M., LAVRENT'EV, YU.G., MAYOROVA, O.N. & POSPELOVA, L.N. (1994): The noble-metal mineralization of the Guli intrusion, Siberian Platform. *Geologia i Geofizika* **9**, 51-65 (in Russ.).
- SHCHEKA, G.G., LEHMANN, B., GIERTH, E., GÖMANN, K. & WALLIANOS, A. (2004): Macrocrystals of Pt-Fe alloy from the Kondyor PGE placer deposit, Khabarovskiy Kray, Russia: trace-element content, mineral inclusions and reaction assemblages. *Can. Mineral.* **42**, 601-617.
- SHCHEKA, S.A., VRZHOSSEK, A.A., SAPIN, V.I. & KIRYUKHINA, N.I. (1991): Transformations of platinum-group minerals from placers of Primorye. *Mineral. Zh.* **13**(13), 34-40 (in Russ.).
- SHNAI, G.K. & KURANOVA, V.N. (1981): New evidence for age of dunite in composite massifs of ultramafic-alkaline composition. *Dokl. Akad. Nauk SSSR* **261**, 950-952 (in Russ.).
- SUSHKIN, L.B. (1995): Characteristic features of native elements of the Konder deposit. *Tikhookeanskaya Geologia* **14**(5), 97-102 (in Russ.).
- ZHERNOVSKY, I.V., MOCHALOV, A.G. & RUDASHEVSKY, N.S. (1985): Phase heterogeneity of isoferroplatinum rich in iron. *Dokl. Akad. Nauk SSSR* **283**, 196-200 (in Russ.).

Received December 1, 2001, revised manuscript accepted March 10, 2005.